

1     **A lipoprotein/ $\beta$ -barrel complex monitors lipopolysaccharide**  
2     **integrity transducing information across the outer membrane.**

3  
4             **Anna Konovalova<sup>1</sup>, Angela M. Mitchell<sup>1</sup>, Thomas J. Silhavy<sup>1,2</sup>**

5  
6     <sup>1</sup>Department of Molecular Biology, Princeton University, Lewis Thomas Laboratory,  
7     Washington Road, Princeton, New Jersey 08544, USA

8     <sup>2</sup> Corresponding author. Email: [tsilhavy@princeton.edu](mailto:tsilhavy@princeton.edu)

9  
10    **Running head:** Lipoprotein RcsF monitors LPS

11  
12    **Keywords:** signal transduction, envelope stress response, Bam complex, polymyxin B,  
13    surface exposed lipoprotein, membrane biogenesis

15   **ABSTRACT**

16   Lipoprotein RcsF is the OM component of the Rcs envelope stress response. RcsF exists  
17   in complexes with  $\beta$ -barrel proteins (OMPs) allowing it to adopt a transmembrane  
18   orientation with a lipidated N-terminal domain on the cell surface and a periplasmic C-  
19   terminal domain. Here we report that mutations that remove BamE or alter a residue in the  
20   RcsF trans-lumen domain specifically prevent assembly of the interlocked complexes  
21   without inactivating either RcsF or the OMP. Using these mutations we demonstrate that  
22   these RcsF/OMP complexes are required for sensing OM outer leaflet stress. Using  
23   mutations that alter the positively charged surface-exposed domain, we show that RcsF  
24   monitors lateral interactions between lipopolysaccharide (LPS) molecules. When these  
25   interactions are disrupted by cationic antimicrobial peptides, or by the loss of negatively  
26   charged phosphate groups on the LPS molecule, this information is transduced to the  
27   RcsF C-terminal signaling domain located in the periplasm to activate the stress response.

28

## 29 INTRODUCTION

30 The outer membrane (OM) of Gram-negative bacteria is an asymmetric bilayer with  
31 lipopolysaccharide (LPS) and phospholipids in the outer and inner leaflets, respectively  
32 (Silhavy et al. 2010). LPS is a glycolipid that consists of three domains: lipid A, the core  
33 and the O-antigen (Raetz and Whitfield 2002). Several sugars in lipid A and the core are  
34 phosphorylated conferring negative charge to the LPS molecule. In the OM, these  
35 negatively charged groups are bridged by divalent cations, which help to establish strong  
36 lateral interactions between LPS molecules. In addition to stabilizing the OM, these lateral  
37 interactions contribute to the unique barrier properties of the OM making it impermeable to  
38 hydrophobic compounds, detergents and dyes (Nikaido 2003). The OM also protects  
39 Gram-negatives from the host innate immunity factors and antibiotics limiting their  
40 effectiveness. In order to disrupt the OM, many organisms produce cationic antibacterial  
41 peptides (CAMPs) that bind LPS (Hancock and Diamond 2000). As a result of this binding,  
42 the OM is permeabilized and this not only facilitates further uptake of the CAMPs but also  
43 sensitizes Gram-negatives to antibiotics and host-factors, including lysozyme. For this  
44 reason, several CAMPs are “last hope” antibiotics against antibiotic-resistant Gram-  
45 negative bacteria (Li et al. 2006).

46 Because of the importance of OM integrity and barrier function for survival, Gram-negative  
47 bacteria have developed several envelope stress responses to monitor and combat  
48 environmental insults. One such envelope response, Rcs (Regulator of Capsule  
49 Synthesis), is activated strongly by OM and PG stress (Majdalani and Gottesman 2005).  
50 Rcs controls the expression of capsule exopolysaccharides that are exported to the cell  
51 surface and help to stabilize the OM (Gottesman et al. 1985). In addition, Rcs  
52 downregulates flagella expression (Francez-Charlot et al. 2003), shifting bacteria from  
53 planktonic to a biofilm growth mode (Ferrieres and Clarke 2003; Latasa et al. 2012), which  
54 is often associated with further increased resistance. Rcs is conserved in

55 *Enterobacteriaceae* and, for many enteric pathogens, it is important for virulence and/or  
56 survival in the host (Erickson and Detweiler 2006; Hinchliffe et al. 2008).

57 Rcs is one of the most complex signal transduction pathways in bacteria involving at least  
58 seven proteins in four different cellular compartments. RcsF is an OM lipoprotein that acts  
59 as a sensory component (Majdalani et al. 2005). Unlike most lipoproteins in *E. coli*, RcsF  
60 is anchored to the outer leaflet of the OM by its lipid moiety and contains an N-terminal  
61 domain that is surface exposed (Konovalova et al. 2014). The short, hydrophilic  
62 transmembrane domain of RcsF is threaded through the lumen of  $\beta$ -barrel proteins  
63 (OMPs) exposing the C-terminal signaling domain in the periplasm (Konovalova et al.  
64 2014). The inner membrane (IM) protein RcsC is a hybrid histidine kinase, which  
65 autophosphorylates and passes the phosphate through the IM phosphotransferase protein  
66 RcsD to a cytoplasmic DNA-binding response regulator RcsB (Stout and Gottesman 1990;  
67 Takeda et al. 2001; Majdalani and Gottesman 2007). RcsB, either alone or in combination  
68 with other regulators, such as RcsA (Stout et al. 1991), BglJ (Venkatesh et al. 2010) or  
69 GadE (Krin et al. 2010) regulates expression of target genes. In addition, IM protein IgaA  
70 negatively regulates the activity of RcsC (Cano et al. 2002; Dominguez-Bernal et al. 2004).

71 Based on genetic analysis as well as some interaction studies it has been proposed that  
72 RcsF can interact directly with the periplasmic domain of IgaA to alleviate inhibition of  
73 RcsC (Dominguez-Bernal et al. 2004; Cho et al. 2014).

74 Although the signal transduction pathway itself is reasonably well characterized, how RcsF  
75 senses the many different envelope defects that induce this system remain poorly  
76 understood. The fact that LPS is found exclusively in the outer leaflet of the OM and that  
77 RcsF is required to sense LPS structural defects prompted us to search for a surface-  
78 exposed domain. Our discovery that RcsF exists in a transmembrane complex with OMPs  
79 suggested that this interlocked structure is required for sensing the LPS defects  
80 (Konovalova et al. 2014). However, another study, which focused primarily on Rcs



81 activated by PG stress caused by A22 or mecillinam treatment, proposed a model in which  
82 the RcsF/OMP complex has no function in RcsF sensing and signaling and only serves an  
83 inhibitory role during steady state growth. This model was based on the observation that  
84 Rcs induction by A22 depends on newly synthesized RcsF (Cho et al. 2014). Here, we  
85 show that the RcsF/OMP complex is functional and that LPS defects are sensed directly  
86 by the surface-exposed domain of RcsF.

87

## 88 **RESULTS**

### 89 **Low levels of polymyxin B cause a specific OM defect**

90 Several mutations in the LPS biosynthesis pathway that result in the production of LPS  
91 molecules with altered structure are known to activate Rcs (Parker et al. 1992). However,  
92 the use of chemical inducers avoids phenotypic adaptation and enables kinetic analysis,  
93 which can provide important insights. Therefore, we sought a small molecule that could be  
94 used to test the function of RcsF/OMP complexes in sensing LPS perturbations.

95 Polymyxin B (PMB) is a CAMP with bactericidal activity and its mechanism of action is well  
96 established (Daugelavicius et al. 2000). When used at the minimal inhibitory concentration  
97 (MIC, 2-8 µg/ml), PMB binds to LPS and destabilizes the OM outer leaflet resulting in  
98 marked increase in OM permeability. When cells are incubated with much higher  
99 concentrations of PMB, it can also integrate into the IM causing a lethal disruption of the  
100 membrane potential. PMB is a known RcsF-dependent inducer of the Rcs pathway (Farris  
101 et al. 2010).

102 In the following experiments, we used 0.5 µg /ml PMB to treat cells in mid-log phase  
103 (OD600 of 0.5,  $5 \times 10^8$  cells/ml). At this cell density, the MIC of PMB was determined to be 8  
104 µg /ml. Therefore, the concentration of PMB we used to induce the Rcs system is more  
105 than 10 fold below the MIC value and growth is not affected under these conditions.

We confirmed that 0.5 µg/ml PMB causes OM, but not IM, stress in our strain background using two routine assays developed to study the effect of CAMPs on the bacterial envelope (Figure 1A and B) (Loh et al. 1984; Wu et al. 1999). The NPN (1-N-phenylnaphthylamine) uptake assay is used to quantitatively monitor OM permeability caused by CAMPs (Loh et al. 1984). NPN is an environmentally sensitive fluorescent dye that fluoresces in the membrane environment but not in solution. Due to its hydrophobic nature, it cannot penetrate Gram-negative OM due to the presence of LPS. However, when CAMPs compromise the OM, NPN enters the cell and integrates into membranes resulting in an increase in fluorescence. When mid-log cells were incubated with 0.5 µg /ml PMB we observed only a small increase in fluorescence, about 1.5 fold, compared to a 6-fold increase when cell were treated with 10 µg /ml PMB (Figure 1A).

The diSC3(5) (Dipropylthiadicarbocyanine iodide) release assay is based on a membrane potential-sensitive fluorescent dye (Wu et al. 1999). DiSC3(5) accumulates in the IM in a proton motive force (PMF)-dependent manner, where it self-quenches the fluorescence. However, when PMF is compromised, diSC3(5) is released from the IM resulting in increased fluorescence. We treated diSC3(5) -labeled cells with 0.5 µg /ml PMB or an MIC (12.5 µg /ml) of Gramicidin, a CAMP known to be PMF uncoupler. Gramicidin A but not PMB caused an increased fluorescence due to diSC3(5) release (Figure 1B). Taken together, these assays demonstrate that at low concentrations PMB does not cause IM depolarization and generates only a small increase in OM permeability, consistent with previous results (Daugelavicius et al. 2000)

We monitored the induction kinetics of the Rcs system in response to PMB using a chromosomal *PrprA-lacZ* reporter fusion (Majdalani et al. 2002). *rprA* encodes a small regulatory RNA that stimulates translation of the mRNA for the stationary phase  $\sigma$  factor RpoS (Majdalani et al. 2002). Expression of *rprA* is regulated exclusive by RcsB and *PrprA-lacZ* is used as a specific reporter for Rcs stress response activation (Majdalani and

Gottesman 2007). For this experiment, we grew the MC4100 *PrprA-lacZ* strain (from now on WT, the parent for all strains) to midlog phase. We then added PMB and followed the Rcs induction over time by monitoring expression of *PrprA-lacZ* reporter using qRT-PCR and  $\beta$ -galactosidase assays. PMB causes a strong and almost immediate induction of Rcs, as quickly as 2 mins on the RNA level and 10 mins on the protein level (Figure 1C).

In order to test whether PMB induces other envelope stress responses or is specific for Rcs, we followed the activity of two other major envelope stress responses, Sigma E and Cpx by monitoring the expression of well-established markers, *rpoE* (Mutalik et al. 2009) and *cpxP* (Danese and Silhavy 1998). Figure 1D shows using qRT-PCR that PMB did not induce either of these stress responses, demonstrating that PMB induces only Rcs.

We also monitored OMP levels during PMB treatment to see whether PMB causes OMP assembly defects. Levels of the three major OMPs did not change upon PMB treatment (Figure 1E). Because we did not observe OMP assembly defects and because the Sigma E response, a sensitive monitor of OMP assembly, was not induced we conclude that low levels of PMB do not inhibit the Bam complex.

Taken together, we conclude that at these sub-MIC levels, PMB causes a specific OM defect.

#### **The PMB-induced Rcs response is independent of *de novo* protein synthesis.**

Globomycin (Glb) is an inhibitor of LspA, the lipoprotein signal peptidase (Inukai et al. 1978; Yamagata et al. 1983; Dev et al. 1985). Glb prevents maturation of lipoproteins resulting in the accumulation of OM lipoproteins in the outer leaflet of the IM. It is well established that, when RcsF accumulates in the outer leaflet of the IM, due to Lol-avoidance mutations that alter the signal sequence or defects in lipoprotein maturation and/or export, it strongly induces the Rcs response (Shiba et al. 2004; Shiba et al. 2012;

Tao et al. 2012). Indeed, we observed strong Rcs induction in response to 5  $\mu$ M Glb (0.5 MIC). This induction required at least 15 mins on the RNA level and 20 mins on the protein level (Figure 1C). Clearly, the kinetics of Rcs induction are much slower with Glb than with PMB. Glb will prevent assembly of essential lipoproteins involved in both LPS and OMP assembly; however, depletion of these proteins to levels low enough to interfere with these assembly processes requires generations (Malinverni et al. 2006; Wu et al. 2006). Indeed, Glb does not induce the Sigma E response even after 60 minutes exposure (Figure 1 – figure supplement 1). Therefore, we conclude that Glb is a chemical inducer of Rcs that is independent of OM damage.

There is no reciprocal transport of lipoproteins from the OM to the IM; therefore, only newly synthesized OM lipoproteins accumulate in the IM under Glb treatment. Therefore, the kinetics of the Glb-induced Rcs response can also serve as a temporal marker for induction due to mislocalization of newly synthesized RcsF. The observation that Glb induced Rcs with slower kinetics than with PMB suggested that induction with PMB does not require newly synthesized RcsF. To test this directly, we used the antibiotic Kasugamycin (Ksg), which is an inhibitor of translation initiation (Okuyama et al. 1971). After 15 mins pre-treatment with Ksg we added PMB or Glb and followed the expression of *PrpA-lacZ* by qRT-PCR (Figure 2). As expected Ksg completely abolished Rcs induction in response to Glb (Figure 2, lower panel), however Ksg did not block the Rcs response to PMB, demonstrating that Rcs induction is independent of *de novo* protein synthesis and does not require newly synthesized RcsF (Figure 2, upper panel). Since RcsF is transported to the OM immediately after it is translocated from the cytoplasm, this result suggests that RcsF molecules already located in the OM are required to respond to PMB treatment.

**RcsF/OMP complexes are required for sensing OM stress.**

RcsF forms an interlocked complex with multiple OMPs, such as OmpA, OmpC and OmpF (Konovalova et al. 2014). However, it is unclear how much uncomplexed RcsF is present in the OM. Since OmpA is the major RcsF-interacting partner (Konovalova et al. 2014), we reasoned that loss of OmpA will lead to significant reduction in RcsF/OMP complexes (Figure 3A and B) and, if this complex senses LPS defects, this reduction should affect the response to PMB but not to Glb.

We followed the kinetics of Rcs induction in response to PMB and Glb in the WT and the *ompA* mutant by monitoring normalized LacZ activity produced by the *PrprA-lacZ* reporter over time (Figure 3C). PMB treatment did not induce Rcs in the *ompA* mutant (Figure. 3C, upper panel). In contrast, Rcs was induced in the *ompA* mutant upon Glb treatment with similar kinetics to that observed for the WT (Figure 3C, lower panel) suggesting that *ompA* is required specifically for PMB-induced OM stress.

OmpA is one of the most abundant OMPs in *E. coli*. To confirm that lack of Rcs response to PMB is the result of loss of RcsF/OMP complexes and not due to damage caused by the loss of the OmpA protein itself, we sought to identify RcsF/OMP assembly defective mutants that would lack RcsF/OmpA complexes but express both the individual proteins. Here we describe two such mutants (Figure 3A and B).

RcsF residue A55 is within the region of RcsF predicted to reside in the lumen of OMPs based on the results of site-specific photo-crosslinking (Figure 3A) (Konovalova et al. 2014). In the course of constructing pBPA variants for site-specific crosslinking, we noticed that the A55-pBPA variant was not functional for LPS sensing and did not crosslink to OMPs. We hypothesized that this residue might be important for RcsF/OMP assembly. Here we report that a mutation *rcsF\_A55Y* results in a significant reduction in the assembly of RcsF/OmpA complexes (Figure 3B, upper panel). Photo-crosslinking also shows that RcsF interacts with BamA and it is thought that this reflects a role for BamA in

207 the assembly of the RcsF/OMP complexes (Konovalova et al. 2014). The *rscF\_A55Y*  
 208 mutation also results in a significant reduction in the levels of RcsF/BamA complex.  
 209 *bamE* encodes one of the non-essential lipoproteins of the Bam complex (Sklar et al.  
 210 2007). *bamE* mutants displayed a striking phenotype in RcsF assembly: levels of  
 211 RcsF/OmpA complexes are severely reduced (Figure 3B, upper panel) and increased  
 212 RcsF/BamA crosslinking is observed (Figure 3B, upper panel). Levels of the individual  
 213 proteins, RcsF, OmpA or BamA, were not affected in these assembly mutants (Figure 3B,  
 214 lower panel).  
 215 Both of the mutants, *rscF\_A55Y* and *bamE*, failed to activate Rcs in response to PMB  
 216 induction (Figure 3C, upper panel); however, both responded to Glb treatment (Figure 3C,  
 217 lower panel). LacZ activity was lower than the WT, likely due to the lower steady state  
 218 levels of LacZ activity in the untreated *rscF\_A55Y* and *bamE* cells.  
 219 To verify that RcsF/OMP complexes are more generally required for sensing LPS-stress  
 220 and not specific to PMB, we tested the effect of the *ompA*, *rscF\_A55Y* and *bamE*  
 221 mutations on Rcs signaling in the LPS biosynthesis mutant *waaP* (*rfaP*) (Figure 3D). *waaP*  
 222 encodes lipopolysaccharide core heptose one (Hep(I) kinase which catalyzes the addition  
 223 of a negatively charged phosphate group to the LPS core (Parker et al. 1992; Yethon et al.  
 224 1998). *waaP* null mutations induce Rcs approximately 8 fold over the WT, resulting in a  
 225 mucoid phenotype (Figure 3 - Figure supplement 2). Deletion of *ompA* in *waaP*  
 226 background resulted in a strong synthetic interaction and this strain had a growth defect in  
 227 liquid culture (Figure 3 - Figure supplement 2). For this reason, we did not perform  
 228 experiments with this strain. When the *rscF\_A55Y* or *bamE* mutation was introduced in the  
 229 *waaP* strain, no growth defect was observed demonstrating that the loss of OmpA not the  
 230 RcsF/OmpA complex causes this synthetic interaction (Figure 3 - Figure supplement 2).  
 231 Strikingly, both assembly mutations significantly reduced the expression of the *PrprA-lacZ*  
 232 reporter in the *waaP* strain and resulted in loss of the mucoid phenotype (Figure 3D,

Figure 3 - Figure supplement 2) indicating that Rcs was not induced. *PrprA-lacZ* expression in the *rcsF\_A55Y* strain was still somewhat stimulated by the *waaP* mutation, likely because the assembly of RcsF/OMP complexes was not completely abolished. Taken together, we conclude that RcsF/OMP complexes are required for sensing LPS defects.

**Positive charge of the surface-exposed region of RcsF is required for LPS-sensing.**

Mutations in several LPS biosynthesis genes result in Rcs induction (Parker et al. 1992). We systematically analyzed the effect of mutations in non-essential genes in the LPS biosynthesis pathway for the ability to induce Rcs (Figure 4A, B). We found mutations that result in defects in inner core biosynthesis and phosphate modification strongly induce Rcs (Figure 4B). *waaCFPG* mutations confer a phenotype, known as a deep rough phenotype; these strains are mucoid and unlike the WT are sensitive to detergents, bile salts and hydrophobic antibiotics (Austin et al. 1990; Kamio and Nikaido 1976; Parker et al. 1992). To differentiate between altered LPS structure and increased permeability as potential inducing signals for Rcs we analyzed several OM biogenesis mutants that also display strong sensitivities to antibiotics without affecting LPS structure.

First, we tested the double *mlaA pldA* mutant, which knocks out two complementary pathways controlling OM lipid asymmetry (Dekker 2000; Malinverni and Silhavy 2009). This mutant has substantially increased levels of phospholipids in the outer leaflet of the OM (Malinverni and Silhavy 2009). Figure 4C shows that Rcs is not induced in this strain. In addition, we tested mutants in the LPS export pathway, *lptD4213* and *lptE\_R91D,K136D* (Ruiz et al. 2005; Malojcic et al. 2014). Rcs was also not induced in these strains (Figure 4C). The permeability phenotype of *lptE\_R91D,K136D* is mild but *mlaA pldA* and *lptD4213* are as sensitive to detergents and hydrophobic antibiotics as deep rough mutants, e.g. *waaP* (Figure 4D). Importantly, RcsF was not generally inhibited in these strains, because it could be activated by introducing the *waaP* mutation (Figure

259 4C). These results demonstrate that OM permeability and/or disrupted asymmetry of the  
260 OM is not a physiological signal for Rcs.

261 The result above suggested that RcsF senses alterations of LPS structure in *waa* mutants  
262 rather than permeability. Mutations in *waaC*, *waaF* and *waaG* result not only in a truncated  
263 core (Figure 4B), but also in the loss of core phosphorylation (Yethon et al. 2000; Yethon  
264 and Whitfield 2001) because the complete inner core with the first glucose is a substrate  
265 for WaaP kinase (Yethon et al. 2000; Yethon and Whitfield 2001). The *waaP* mutation  
266 does not introduce core truncations but results in the loss of a majority of these core  
267 phosphates because WaaP activity is a prerequisite for WaaY phosphorylation of Hep(II)  
268 (Yethon et al. 1998). Our results demonstrate that *waaP* mutation and therefore decreased  
269 phosphorylation of LPS is sufficient to fully induce Rcs (Figure 4B).

270 LPS phosphates are essential for establishing cation-mediated LPS cross-bridges in the  
271 OM. LB is a  $Mg^{2+}$ -limiting medium, and does not contain a sufficient amount of cations to  
272 saturate LPS (Papp-Wallace and Maguire 2008; Nikaido 2009). Addition of  $Mg^{2+}$  is known  
273 to stabilize the OM of the deep rough mutants (Chatterjee et al., 1976), likely through  
274 stabilization of the lipid A phosphates. Interestingly, when 10 mM  $Mg^{2+}$  was added to LB, it  
275 decreased Rcs induction in *waaP* mutant (Figure 4E).

276 The two-component PhoPQ system responds to low  $Mg^{2+}$  concentrations (Soncini et al.  
277 1996; Kato et al. 2003). PhoPQ and Rcs are known to have partially overlapping regulons  
278 in several enterobacteria (Hagiwara et al. 2003; Garcia-Calderon et al. 2007). Unlike in  
279 *Salmonella*, PhoPQ in *E. coli* does not regulate lipid A modifications through the Pmr  
280 pathway (Winfield and Groisman 2004; Rubin et al. 2015). Because we observed a  $Mg^{2+}$   
281 dependent effect on Rcs in a *waaP* mutant, we analyzed Rcs induction in *waaP phoP*  
282 mutant (Figure 4E). Rcs was still induced and responded to  $Mg^{2+}$ -addition in the *waaP*  
283 *phoP* mutant (Figure 4E). Therefore, we concluded that  $Mg^{2+}$  dependent Rcs signaling in



284 *waaP* mutants was independent of PhoPQ and is likely a result of reinforced cross-bridges  
285 between lipid A-phosphates.

286 The effect of LPS charge and presence of cations on Rcs signaling lead us to suggest that  
287 RcsF senses the strength of LPS lateral interactions. Binding of a cationic peptide, such as  
288 PMB to LPS would also neutralize the charge and weaken LPS lateral interactions. PMB  
289 also contains lipid in addition to a cyclic peptide ring, and the lipid integrates into and can  
290 disorganize the membrane bilayer (Vaara 1992) . We therefore tested whether charge-  
291 neutralization of LPS by PMB is sufficient to induce Rcs. For this, we analyzed the ability  
292 of a lipid-truncated PMB derivative, PMB nonapeptide (PMBN) to induce Rcs. PMBN also  
293 neutralizes LPS but does not disturb the bilayer and is non-toxic. Like PMB, PMBN also  
294 induces Rcs, but higher concentrations are required to offset the lower affinity of binding to  
295 LPS (Figure 4F) (Vaara and Viljanen 1985; Thomas and Surolia 1999). Therefore, we  
296 conclude that charge-neutralization of LPS by PMB is sufficient to induce Rcs.

297 If RcsF/OMP complexes sense LPS defects directly, it seems likely that the surface-  
298 exposed domain of RcsF acts as the sensory domain. One of the interesting features of  
299 surface-exposed region of RcsF is the abundance of positively charged amino acids  
300 (Figure 5A). To investigate the role of these positive charges in sensing LPS defects, we  
301 substituted the five Arg and Lys residues in the surface-exposed region (16-48) with Ala to  
302 generate a charge substitution mutant gene we refer to as *rcsF\_A5* (Figure 5A). We  
303 verified that RcsF/OmpA complexes are formed with the same efficiency as in RcsF\_WT  
304 (Figure 5B) and that this mutant protein responded normally to Glb (Figure 5C, lower  
305 panel). Next, we tested how this mutant protein responded to PMB (Figure 5C, upper  
306 panel). Although not completely abolished, the Rcs response to PMB was significantly  
307 reduced as compared to WT (Figure 5C, upper panel). Likewise, introduction of *rcsF\_A5*  
308 into the *waaP* background results in significantly reduced expression of *PrprA-lacZ* and  
309 loss of the mucoid phenotype (Figure 5D, Figure 5 – Figure supplement 2). We conclude

that the positive charge of surface-exposed region of RcsF is important for sensing alterations in LPS.

## DISCUSSION

The lipidated amino terminus of lipoprotein RcsF is displayed on the cell surface; the carboxy-terminal signaling domain resides in the periplasm and the short, hydrophilic transmembrane domain is protected from the lipid environment by threading through an OMP, most often OmpA. We show here that this interlocked, heterodimeric structure functions directly to sense known Rcs inducing signals that cause perturbations in the outer leaflet of the OM caused either by treatment with CAMPs or by mutations that cause LPS structural defects. We show that altered OM permeability or asymmetry are not physiological inducers of RcsF. Instead, RcsF senses the state of LPS lateral interactions and it is activated when these interactions are perturbed either by: i) neutralization of LPS negative charge by CAMPs (such as PMB) as a result of direct binding; ii) decreased LPS phosphorylation as a result of mutations in LPS biosynthesis pathway; iii) by lack of cations to stabilize LPS cross-bridges. Moreover, we show that the positive charge of surface-exposed domain of RcsF is necessary for sensing these LPS defects.

An alternative model for RcsF signaling has been proposed by Cho et al., 2014. This model proposes that in unstressed cells, RcsF is constantly assembled into RcsF/OmpA complexes that have no function in sensing and signal transduction. Signals that induce Rcs do so by inhibiting the function of the Bam complex. This prevents RcsF/OMP assembly and allows newly synthesized RcsF to remain free in the periplasm where it can engage the IM components of the signal transduction system. According to this model, activation of Rcs signaling depends on *de novo* protein synthesis (Cho et al. 2014).

334 Here, we have provided multiple lines of evidence demonstrating that this model cannot  
335 explain how RcsF senses changes in the OM outer leaflet. First, as noted above, we show  
336 that the surface-exposed domain of RcsF/OmpA functions directly to sense these defects.  
337 Second, we provide evidence that PMB does not affect  $\beta$ -barrel assembly nor does it  
338 induce the SigmaE stress response, which is a sensitive indicator of Bam complex function  
339 and the presence of unfolded OMPs in the periplasm. Finally, we show that PMB induction  
340 of the Rcs system happens even in the presence of a protein synthesis inhibitor.

341 Two other categories of mutations or chemical agents are also known Rcs inducers: i)  
342 perturbations affecting lipoprotein maturation, such as *pgsA* (Shiba et al. 2004), Glb (this  
343 study), or trafficking (*lolA* depletion) (Tao et al. 2012); ii) perturbations in PG biogenesis,  
344 such as those caused by treatment with mecillinam and other  $\beta$ -lactams (Laubacher and  
345 Ades 2008), lysozyme (Callewaert et al. 2009; Ranjit and Young 2013), A22 (Cho et al.  
346 2014), or genetically by introducing multiple *pbp* knockouts (*pbp4*, 5, 7, *ampH*) (Evans et  
347 al. 2013).

348 It is well established that perturbations in lipoprotein assembly lead to the accumulation of  
349 RcsF in the inner membrane allowing interaction with downstream components (Shiba et  
350 al. 2012). Using Ksg, we show that this mechanism clearly depends on RcsF *de novo*  
351 synthesis and is independent of RcsF/OMP assembly in the OM.

352 Activation of RcsF in response to perturbations in PG biogenesis also depends on protein  
353 synthesis and is likely independent of RcsF/OMP complexes (Cho et al. 2014). However, it  
354 is unclear how PG defects induce Rcs. RcsF does not interact with PG, and therefore,  
355 activation might not be direct. For example,  $\beta$ -lactams (including mecillinam), A22 and  
356 mutations in *pbp* genes induce not only Rcs but also the Cpx response (Laubacher and  
357 Ades 2008; Delhay, Collet et al. 2016; Evans et al. 2013) and, at least in the case of the  
358 *pbp4*, 5, 7, and *ampH* mutations, Rcs induction relies fully on Cpx (Evans et al. 2013).  
359 Because A22 and mecillinam treatment decrease RcsF/BamA crosslinking, it was

proposed that RcsF monitors the activity of the Bam complex (Cho et al. 2014). However, there is no evidence that any of the treatments that affect PG affect the function of the Bam complex. We propose an alternative explanation in which newly synthesized RcsF is engaged in signaling prior its interactions with BamA. Reduction of RcsF/OMP complexes may facilitate this type of signaling by increasing proportion of periplasmic RcsF.

Our work also provides important insights into the assembly pathway for the remarkable, interlocked RcsF/OMP complexes. The first of these relates to BamE. *bamE* encodes one of the non-essential lipoproteins of the Bam complex (Sklar et al. 2007), and the function of BamE is not well-understood. Recent studies have uncovered a role for BamE in modulating BamA activity (Rigel et al. 2012; Rigel et al. 2013). However, *bamE* null mutations confer modest phenotypes with only slight defects in OMP assembly (Sklar et al. 2007; Rigel et al. 2012). Here, we show that BamE plays an essential role in assembly of RcsF/OMP complexes. In a strain lacking BamE, RcsF/OmpA complexes are almost undetectable. Nonetheless, RcsF is still recognized by BamA. In fact, increased RcsF/BamA crosslinking is observed in a *bamE* strain. This finding further supports the model that RcsF/BamA crosslinking represents an intermediate in RcsF/OMP assembly pathway and suggests that RcsF binds BamA before it binds the OMP.

Secondly, we identified a mutation, *rscF\_A55Y* that alters a trans-lumen residue and inhibits assembly of RcsF into OMP complexes. We showed that the A55Y substitution prevents RcsF binding to BamA and this in turn prevents assembly of the RcsF/OMP complex. It is important to note that this mutation does not affect the interactions between RcsF and the downstream signaling components, as the *rscF\_A55Y* mutant protein was still able to activate Rcs in response to Glb.

We do not yet understand how the inducing signal is transduced by the RcsF/OMP complexes from the cell surface to the IM components of the Rcs system. The RcsF/OMP complexes do not disassemble when OM defects are detected. Therefore, we hypothesize

386 that small conformational changes within complex can facilitate interaction between the  
387 RcsF carboxy-terminal signaling domain and the downstream components to activate the  
388 signaling pathway and we are currently attempting to detect these changes in the  
389 RcsF/OMP complexes in response to LPS defects.

390

## MATERIALS AND METHODS

### Strain growth and construction.

All strains used in this study, including previously published strains (Majdalani et al. 2002, Malinverni et al. 2006, Malojcic et al. 2014, Silhavy et al. 1984) are listed in Supplementary file 1. Strains were grown in LB (10 g/L tryptone, 5 g/L yeast extract, 10 g/L NaCl) at 37 °C. LB was supplemented with 10 mM MgSO<sub>4</sub> when indicated. Arabinose was added at the final concentration of 0.2% to support growth of *lptE\_R91D K136D* mutant. Antibiotics were added when appropriate at the following concentration: chloramphenicol 20 µg/ml, kanamycin 25 µg/ml, tetracycline 20 µg/ml. Strains were generated by P1vir transduction (Silhavy et al. 1984). The kanamycin resistance cassette was cured from Keio derived mutants with plasmid pCP20, as previously described (Datsenko and Wanner 2000).

### NPN uptake assay.

NPN uptake assay was performed according to (Loh et al. 1984). Briefly, AK-265 strain was grown to an OD<sub>600</sub> of 0.5, cells were collected by centrifugation and washed twice with 5 mM HEPES, pH 7.2. Cells were resuspended to OD<sub>600</sub>=0.5 and NPN (1-N-phenylnaphthylamine, Sigma) was added to a final concentration of 10 µM. 200 µl of cell suspension was pipetted into wells of black 96 well plates. PMB was added to a final concentration of 0.5 or 8 µg/ml. Fluorescence (excitation 350 nm/emission 420 nm) was measured for 10 mins with 1 min interval using BioTek Synergy 1 plate reader. Endpoint fluorescence was normalized as a fold of untreated sample (vehicle control) and values represent mean with SD between three independent measurements.

### diSC3(5) release assay.

diSC3(5) (Sigma) release assay was performed following the protocol by (Zhang et al. 2000a) but adopted for a plate-reader format. Briefly, AK-265 strain was grown to an OD<sub>600</sub> of 0.5, cells were collected by centrifugation and washed twice with 5 mM HEPES, pH 7.8. Cells were resuspended to OD<sub>600</sub>=0.05 in 5 mM HEPES, pH 7.8 with 0.2 mM

EDTA. diSC3(5) was added to the final concentration of 0.4  $\mu$ M. 180  $\mu$ l of cell suspension was pipetted into wells of black 96 well plates. Uptake of diSC3(5) dye was monitored by a decrease in fluorescence excitation 622 nm/emission 670 nm using BioTek Synergy 1 plate reader. After fluorescence signal reached steady state (appr. 30 mins), 20  $\mu$ l of 1 M KCl solution was added to equilibrate the cytoplasmic and external K<sup>+</sup> concentrations. PMB or gramicidin (Sigma) was added where applicable to the final concentration of 0.5 and 12.5  $\mu$ g/ml, respectively, and incubated for 15 mins. Fluorescence was measured and normalized as a fold of untreated sample (vehicle control) and values represent mean with SD between three independent measurements.

#### **Quantification of RNA induction by qRT-PCR**

For analysis of RNA level induction of Rcs, overnight cultures of AK-265 were back diluted to  $2 \times 10^7$  cells/ml and grown to an OD600 of 0.5. Where applicable, cultures were then treated with 500  $\mu$ g/ml Ksg or a vehicle control for 15 minutes. Cultures were then treated with 0.5  $\mu$ g/ml PMB or 5  $\mu$ M Glb. Samples for RNA analysis were harvested at the indicated time points and immediately fixed with a 2X volume of RNAProtect Bacterial Reagent (Qiagen) as per manufacturer instructions. The fixed cells were lysed and RNA was harvested using the RNeasy kit (Qiagen) with on column DNase (Qiagen) digestion as per manufacturer instructions. The RNA was quantitated using a Synergy H1 Hybrid Reader (BioTek) and cDNA was synthesized from 1  $\mu$ g of RNA using a High Capacity cDNA reverse transcription kit (Thermo Fisher Scientific) in a 20  $\mu$ l reaction.

For qPCR, 10  $\mu$ l reactions were run in triplicate using PerfecCTa SYBR Green FastMix R0X (Quanta Biosciences), 0.5  $\mu$ M primers, and 2  $\mu$ l of a 1:500 dilution of cDNA samples.

The following primers were utilized to quantitate *lacZ* (left: 5'-GAAAGCTGGCTACAGGAA-3'; right 5'-GCAGCAACGAGACGTCA-3'), *rpoE* (left: 5'-

TGGCCTGAGCTATGAAGAGATAG-3', right: 5'CCTGATAAGCGGTTGAACTTTG-3'

(Denoncin et al. 2012)), *cpxP* (left: 5'-TGCTGAAGTCGGTTCAGGCGATAA-3', Right: 5'-

TCTGCTGACGCTGATGTTTCGGTTA-3'), *nrdR* (left: 5'-ATGCATTGCCATTCTGTTT-3',

right: 5'-CCGCTACGCAATTTCTCTTC-3'), and *ubiJ* (left: 5'-  
GTTATCGCCTACGCCAGTGT-3', 5'-GGCTTTGCTGATTCCTTCAG-3'). RNA expression  
of *rprA* was not directly analyzed as high levels of secondary structure prevent accurate  
quantification by qRT-PCR (data not shown). The qPCR reactions were run on the  
StepOne Plus RealTime PCR System (Thermo Fisher Scientific) using the StepOne  
Software V2.3 (Thermo Fisher Scientific) on the following program: 95 °C for 10 minutes,  
followed by 40 cycles of 95°C for 15 s, 60°C for 1 min (acquisition). Absolute quantification  
for each primer set was performed based on Ct values calculated by automatic  
thresholding compared to a standard curve of  $10^1$  to  $10^7$  copies per reaction of *E. coli* K12  
MG1655 genomic DNA. Relative expression of *lacZ*, *rpoE*, and *cpxP* was calculated using  
*nrdR* (Figure 2A) and *ubiJ* (Figure 2B & C) as endogenous control genes, as they have  
been found to be invariant in a wide range of conditions (Heng et al. 2011). For calculating  
fold induction, relative expression values were normalized a no treatment control for each  
time point. The kinetics of *lacZ* induction (Figure 1C upper panel) are indicated as a  
representative experiment with error bars representing one standard deviation. Other qRT-  
PCR experiments (Figure 1D and Figure 2) are indicated as the mean of three  
independent biological replicates+/-SEM.

#### ***In vivo* formaldehyde crosslinking.**

Strains were grown to an OD600 of 0.5-0.7, washed twice in PBS (Na<sub>2</sub>HPO<sub>4</sub> 10mM,  
KH<sub>2</sub>PO<sub>4</sub> 1.8 mM, KCl 2.7 mM, NaCl 137 mM, pH 7.6) and concentrated to OD600=10 in  
PBS. Formaldehyde was added to the final concentration of 0.7% and crosslinked for 12  
mins at room temperature. Crosslinking was stopped by adding of Tris-Cl (100 mM final);  
cells were collected by centrifugation and suspended in SDS loading buffer. Samples were  
heated at 65 C for 15 mins and analyzed by immune blotting with anti-RcsF antibodies.

#### **β-galactosidase assay**

For a time course experiments, overnight cultures of corresponding strains were diluted  
1:100 in LB (supplemented with kanamycin 25 µg/ml when needed) and grown to an



OD600 of 0.5 in a shaking water bath at 37 °C. Cultures were then treated with 0.5 µg/ml PMB or 5 µM Glb for a course of 60 mins. Samples were taken every 10 mins for a β-galactosidase assay and for OD600 measurement. For a β-galactosidase assay, 100 µl samples were taken and added directly to 900 µl of Z buffer (60 mM Na<sub>2</sub>HPO<sub>4</sub>, 40 mM NaH<sub>2</sub>PO<sub>4</sub>, 10 mM KCl, 1 mM MgSO<sub>4</sub>, 50 mM β-mercaptoethanol, 0.03% SDS). 50 µl of chloroform was added to stop growth and mix vigorously by pipetting. After collecting all samples, 100 µl of cell each lysate was mixed with 100 µl of 4 mg/ml O-nitrophenyl-β-D-galactopyranoside (ONPG) solution in Z buffer. β-galactosidase activity was analyzed by a kinetic measurement of OD420 in a BioTek Synergy 1 plate reader and Vmax was determined using Gen5 software. Vmax was normalized by OD600. Experiments were performed in three biological replicates and mean values +/- SEM were plotted. Graphs were built by GraphPad Prism 6 software. For a single point measurement, corresponding strains were grown to an OD600 of 0.5-0.7 and samples for a β-galactosidase assay were taken and analyzed as described above.

## ACKNOWLEDGEMENTS

We thank members of the Silhavy lab for helpful discussions and the feedback on the manuscript. This work was supported by National Institute of General Medical Sciences Grant GM34821 (to T.J.S.).

## REFERENCES

- Austin EA, Graves JF, Hite LA, Parker CT, Schnaitman CA. 1990. Genetic analysis of lipopolysaccharide core biosynthesis by *Escherichia coli* K-12: insertion mutagenesis of the *rfa* locus. *J Bacteriol* **172**: 5312-5325.
- Callewaert L, Vanoirbeek KG, Lurquin I, Michiels CW, Aertsen A. 2009. The Rcs two-component system regulates expression of lysozyme inhibitors and is induced by exposure to lysozyme. *J Bacteriol* **191**: 1979-1981.
- Cano DA, Dominguez-Bernal G, Tierrez A, Garcia-Del Portillo F, Casadesus J. 2002. Regulation of capsule synthesis and cell motility in *Salmonella enterica* by the essential gene *igaA*. *Genetics* **162**: 1513-1523.
- Cho SH, Szewczyk J, Pesavento C, Zietek M, Banzhaf M, Roszczenko P, Asmar A, Laloux G, Hov AK, Leverrier P et al. 2014. Detecting envelope stress by monitoring beta-barrel assembly. *Cell* **159**: 1652-1664.
- Danese PN, Silhavy TJ. 1998. CpxP, a stress-combative member of the Cpx regulon. *J Bacteriol* **180**: 831-839.
- Datsenko KA, Wanner BL. 2000. One-step inactivation of chromosomal genes in *Escherichia coli* K-12 using PCR products. *Proc Natl Acad Sci U S A* **97**: 6640-6645.
- Daugelavicius R, Bakiene E, Bamford DH. 2000. Stages of polymyxin B interaction with the *Escherichia coli* cell envelope. *Antimicrob Agents Chemother* **44**: 2969-2978.
- Dekker N. 2000. Outer-membrane phospholipase A: known structure, unknown biological function. *Mol Microbiol* **35**: 711-717.
- Delhaye, A., J. F. Collet and G. Laloux (2016). "Fine-Tuning of the Cpx Envelope Stress Response Is Required for Cell Wall Homeostasis in *Escherichia coli*." *MBio* **7**(1): e00047-00016.

516 Denoncin K, Schwalm J, Vertommen D, Silhavy TJ, Collet JF. 2012. Dissecting the  
 517 Escherichia coli periplasmic chaperone network using differential proteomics.  
 518 *Proteomics* **12**: 1391-1401.

519 Dev IK, Harvey RJ, Ray PH. 1985. Inhibition of prolipoprotein signal peptidase by  
 520 globomycin. *J Biol Chem* **260**: 5891-5894.

521 Dominguez-Bernal G, Pucciarelli MG, Ramos-Morales F, Garcia-Quintanilla M, Cano DA,  
 522 Casadesus J, Garcia-del Portillo F. 2004. Repression of the RcsC-YojN-RcsB  
 523 phosphorelay by the IgaA protein is a requisite for Salmonella virulence. *Mol*  
 524 *Microbiol* **53**: 1437-1449.

525 Erickson KD, Detweiler CS. 2006. The Rcs phosphorelay system is specific to enteric  
 526 pathogens/commensals and activates ydeI, a gene important for persistent  
 527 Salmonella infection of mice. *Mol Microbiol* **62**: 883-894.

528 Evans KL, Kannan S, Li G, de Pedro MA, Young KD. 2013. Eliminating a set of four  
 529 penicillin binding proteins triggers the Rcs phosphorelay and Cpx stress responses  
 530 in Escherichia coli. *J Bacteriol* **195**: 4415-4424.

531 Farris C, Sanowar S, Bader MW, Pfuetzner R, Miller SI. 2010. Antimicrobial peptides  
 532 activate the Rcs regulon through the outer membrane lipoprotein RcsF. *J Bacteriol*  
 533 **192**: 4894-4903.

534 Ferrieres L, Clarke DJ. 2003. The RcsC sensor kinase is required for normal biofilm  
 535 formation in Escherichia coli K-12 and controls the expression of a regulon in  
 536 response to growth on a solid surface. *Mol Microbiol* **50**: 1665-1682.

537 Francez-Charlot A, Laugel B, Van Gemert A, Dubarry N, Wiorowski F, Castanie-Cornet  
 538 MP, Gutierrez C, Cam K. 2003. RcsCDB His-Asp phosphorelay system negatively  
 539 regulates the flhDC operon in Escherichia coli. *Mol Microbiol* **49**: 823-832.

540 Garcia-Calderon CB, Casadesus J, Ramos-Morales F. 2007. Rcs and PhoPQ regulatory  
 541 overlap in the control of Salmonella enterica virulence. *J Bacteriol* **189**: 6635-6644.

542 Gottesman S, Trisler P, Torres-Cabassa A. 1985. Regulation of capsular polysaccharide  
543 synthesis in Escherichia coli K-12: characterization of three regulatory genes. *J*  
544 *Bacteriol* **162**: 1111-1119.

545 Hagiwara D, Sugiura M, Oshima T, Mori H, Aiba H, Yamashino T, Mizuno T. 2003.  
546 Genome-wide analyses revealing a signaling network of the RcsC-YojN-RcsB  
547 phosphorelay system in Escherichia coli. *J Bacteriol* **185**: 5735-5746.

548 Hancock RE, Diamond G. 2000. The role of cationic antimicrobial peptides in innate host  
549 defences. *Trends Microbiol* **8**: 402-410.

550 Heng SS, Chan OY, Keng BM, Ling MH. 2011. Glucan Biosynthesis Protein G Is a  
551 Suitable Reference Gene in Escherichia coli K-12. *ISRN Microbiol* **2011**: 469053.

552 Hinchliffe SJ, Howard SL, Huang YH, Clarke DJ, Wren BW. 2008. The importance of the  
553 Rcs phosphorelay in the survival and pathogenesis of the enteropathogenic  
554 yersiniae. *Microbiology* **154**: 1117-1131.

555 Inukai M, Takeuchi M, Shimizu K, Arai M. 1978. Mechanism of action of globomycin. *J*  
556 *Antibiot (Tokyo)* **31**: 1203-1205.

557 Kamio Y, Nikaido H. 1976. Outer membrane of Salmonella typhimurium: accessibility of  
558 phospholipid head groups to phospholipase c and cyanogen bromide activated  
559 dextran in the external medium. *Biochemistry* **15**: 2561-2570.

560 Kato A, Latifi T, Groisman EA. 2003. Closing the loop: the PmrA/PmrB two-component  
561 system negatively controls expression of its posttranscriptional activator PmrD. *Proc*  
562 *Natl Acad Sci U S A* **100**: 4706-4711.

563 Konovalova A, Perlman DH, Cowles CE, Silhavy TJ. 2014. Transmembrane domain of  
564 surface-exposed outer membrane lipoprotein RcsF is threaded through the lumen  
565 of beta-barrel proteins. *Proc Natl Acad Sci U S A* **111**: E4350-4358.

566 Krin E, Danchin A, Soutourina O. 2010. RcsB plays a central role in H-NS-dependent  
567 regulation of motility and acid stress resistance in Escherichia coli. *Res Microbiol*  
568 **161**: 363-371.

569 Latasa C, Garcia B, Echeverz M, Toledo-Arana A, Valle J, Campoy S, Garcia-del Portillo  
 570 F, Solano C, Lasa I. 2012. Salmonella biofilm development depends on the  
 571 phosphorylation status of RcsB. *J Bacteriol* **194**: 3708-3722.

572 Laubacher ME, Ades SE. 2008. The Rcs phosphorelay is a cell envelope stress response  
 573 activated by peptidoglycan stress and contributes to intrinsic antibiotic resistance. *J*  
 574 *Bacteriol* **190**: 2065-2074.

575 Li J, Nation RL, Turnidge JD, Milne RW, Coulthard K, Rayner CR, Paterson DL. 2006.  
 576 Colistin: the re-emerging antibiotic for multidrug-resistant Gram-negative bacterial  
 577 infections. *The Lancet Infectious Diseases* **6**: 589-601.

578 Loh B, Grant C, Hancock RE. 1984. Use of the fluorescent probe 1-N-  
 579 phenylmethylamine to study the interactions of aminoglycoside antibiotics with the  
 580 outer membrane of *Pseudomonas aeruginosa*. *Antimicrob Agents Chemother* **26**:  
 581 546-551.

582 Majdalani N, Gottesman S. 2005. The Rcs phosphorelay: a complex signal transduction  
 583 system. *Annu Rev Microbiol* **59**: 379-405.

584 Majdalani N, Gottesman S. 2007. Genetic dissection of signaling through the Rcs  
 585 phosphorelay. *Methods Enzymol* **423**: 349-362.

586 Majdalani N, Heck M, Stout V, Gottesman S. 2005. Role of RcsF in signaling to the Rcs  
 587 phosphorelay pathway in *Escherichia coli*. *J Bacteriol* **187**: 6770-6778.

588 Majdalani N, Hernandez D, Gottesman S. 2002. Regulation and mode of action of the  
 589 second small RNA activator of RpoS translation, RprA. *Mol Microbiol* **46**: 813-826.

590 Malinverni JC, Silhavy TJ. 2009. An ABC transport system that maintains lipid asymmetry  
 591 in the gram-negative outer membrane. *Proc Natl Acad Sci U S A* **106**: 8009-8014.

592 Malinverni JC, Werner J, Kim S, Sklar JG, Kahne D, Misra R, Silhavy TJ. 2006. YfiO  
 593 stabilizes the YaeT complex and is essential for outer membrane protein assembly  
 594 in *Escherichia coli*. *Mol Microbiol* **61**: 151-164.

595 Malojcic G, Andres D, Grabowicz M, George AH, Ruiz N, Silhavy TJ, Kahne D. 2014. LptE  
 596 binds to and alters the physical state of LPS to catalyze its assembly at the cell  
 597 surface. *Proc Natl Acad Sci U S A* **111**: 9467-9472.

598 Mutalik VK, Nonaka G, Ades SE, Rhodius VA, Gross CA. 2009. Promoter strength  
 599 properties of the complete sigma E regulon of Escherichia coli and Salmonella  
 600 enterica. *J Bacteriol* **191**: 7279-7287.

601 Nikaido H. 2003. Molecular basis of bacterial outer membrane permeability revisited.  
 602 *Microbiol Mol Biol Rev* **67**: 593-656.

603 Nikaido H. 2009. The Limitations of LB Medium.  
 604 [http://schaechter.asmblog.org/schaechter/2009/2011/the-limitations-of-lb-](http://schaechter.asmblog.org/schaechter/2009/2011/the-limitations-of-lb-medium.html)  
 605 [medium.html](http://schaechter.asmblog.org/schaechter/2009/2011/the-limitations-of-lb-medium.html).

606 Okuyama A, Machiyama N, Kinoshita T, Tanaka N. 1971. Inhibition by kasugamycin of  
 607 initiation complex formation on 30S ribosomes. *Biochem Biophys Res Commun* **43**:  
 608 196-199.

609 Papp-Wallace KM, Maguire ME. 2008. Magnesium Transport and Magnesium  
 610 Homeostasis. *EcoSal Plus* **3**.

611 Parker CT, Kloser AW, Schnaitman CA, Stein MA, Gottesman S, Gibson BW. 1992. Role  
 612 of the rfaG and rfaP genes in determining the lipopolysaccharide core structure and  
 613 cell surface properties of Escherichia coli K-12. *J Bacteriol* **174**: 2525-2538.

614 Raetz CR, Whitfield C. 2002. Lipopolysaccharide endotoxins. *Annu Rev Biochem* **71**: 635-  
 615 700.

616 Ranjit DK, Young KD. 2013. The Rcs stress response and accessory envelope proteins  
 617 are required for de novo generation of cell shape in Escherichia coli. *J Bacteriol*  
 618 **195**: 2452-2462.

619 Rigel NW, Ricci DP, Silhavy TJ. 2013. Conformation-specific labeling of BamA and  
 620 suppressor analysis suggest a cyclic mechanism for beta-barrel assembly in  
 621 Escherichia coli. *Proc Natl Acad Sci U S A* **110**: 5151-5156.

622 Rigel NW, Schwalm J, Ricci DP, Silhavy TJ. 2012. BamE modulates the Escherichia coli  
623 beta-barrel assembly machine component BamA. *J Bacteriol* **194**: 1002-1008.

624 Rubin EJ, Herrera CM, Crofts AA, Trent MS. 2015. PmrD is required for modifications to  
625 escherichia coli endotoxin that promote antimicrobial resistance. *Antimicrob Agents*  
626 *Chemother* **59**: 2051-2061.

627 Ruiz N, Falcone B, Kahne D, Silhavy TJ. 2005. Chemical conditionality: a genetic strategy  
628 to probe organelle assembly. *Cell* **121**: 307-317.

629 Shiba Y, Miyagawa H, Nagahama H, Matsumoto K, Kondo D, Matsuoka S, Hara H. 2012.  
630 Exploring the relationship between lipoprotein mislocalization and activation of the  
631 Rcs signal transduction system in Escherichia coli. *Microbiology* **158**: 1238-1248.

632 Shiba Y, Yokoyama Y, Aono Y, Kiuchi T, Kusaka J, Matsumoto K, Hara H. 2004.  
633 Activation of the Rcs signal transduction system is responsible for the  
634 thermosensitive growth defect of an Escherichia coli mutant lacking  
635 phosphatidylglycerol and cardiolipin. *J Bacteriol* **186**: 6526-6535.

636 Silhavy TJ, Berman ML, Enquist LW, Cold Spring Harbor Laboratory. 1984. *Experiments*  
637 *with gene fusions*. Cold Spring Harbor Laboratory, Cold Spring Harbor, N.Y.

638 Silhavy TJ, Kahne D, Walker S. 2010. The bacterial cell envelope. *Cold Spring Harb*  
639 *Perspect Biol* **2**: a000414.

640 Sklar JG, Wu T, Gronenberg LS, Malinverni JC, Kahne D, Silhavy TJ. 2007. Lipoprotein  
641 SmpA is a component of the YaeT complex that assembles outer membrane  
642 proteins in Escherichia coli. *Proc Natl Acad Sci U S A* **104**: 6400-6405.

643 Soncini FC, Garcia Vescovi E, Solomon F, Groisman EA. 1996. Molecular basis of the  
644 magnesium deprivation response in Salmonella typhimurium: identification of PhoP-  
645 regulated genes. *J Bacteriol* **178**: 5092-5099.

646 Stout V, Gottesman S. 1990. RcsB and RcsC: a two-component regulator of capsule  
647 synthesis in Escherichia coli. *J Bacteriol* **172**: 659-669.

648 Stout V, Torres-Cabassa A, Maurizi MR, Gutnick D, Gottesman S. 1991. RcsA, an  
649 unstable positive regulator of capsular polysaccharide synthesis. *J Bacteriol* **173**:  
650 1738-1747.

651 Takeda S, Fujisawa Y, Matsubara M, Aiba H, Mizuno T. 2001. A novel feature of the  
652 multistep phosphorelay in Escherichia coli: a revised model of the RcsC --> YojN --  
653 > RcsB signalling pathway implicated in capsular synthesis and swarming  
654 behaviour. *Mol Microbiol* **40**: 440-450.

655 Tao K, Narita S, Tokuda H. 2012. Defective lipoprotein sorting induces lolA expression  
656 through the Rcs stress response phosphorelay system. *J Bacteriol* **194**: 3643-3650.

657 Thomas CJ, Surolia A. 1999. Kinetics of the interaction of endotoxin with polymyxin B and  
658 its analogs: a surface plasmon resonance analysis. *FEBS Lett* **445**: 420-424.

659 Vaara M. 1992. Agents that increase the permeability of the outer membrane. *Microbiol*  
660 *Rev* **56**: 395-411.

661 Vaara M, Viljanen P. 1985. Binding of polymyxin B nonapeptide to gram-negative bacteria.  
662 *Antimicrob Agents Chemother* **27**: 548-554.

663 Venkatesh GR, Kembou Koungni FC, Paukner A, Stratmann T, Blissenbach B, Schnetz K.  
664 2010. BglJ-RcsB heterodimers relieve repression of the Escherichia coli bgl operon  
665 by H-NS. *J Bacteriol* **192**: 6456-6464.

666 Winfield MD, Groisman EA. 2004. Phenotypic differences between Salmonella and  
667 Escherichia coli resulting from the disparate regulation of homologous genes. *Proc*  
668 *Natl Acad Sci U S A* **101**: 17162-17167.

669 Wu M, Maier E, Benz R, Hancock RE. 1999. Mechanism of interaction of different classes  
670 of cationic antimicrobial peptides with planar bilayers and with the cytoplasmic  
671 membrane of Escherichia coli. *Biochemistry* **38**: 7235-7242.

672 Wu T, McCandlish AC, Gronenberg LS, Chng SS, Silhavy TJ, Kahne D. 2006.  
673 Identification of a protein complex that assembles lipopolysaccharide in the outer  
674 membrane of Escherichia coli. *Proc Natl Acad Sci U S A* **103**: 11754-11759.



675 Yamagata H, Taguchi N, Daishima K, Mizushima S. 1983. Genetic characterization of a  
676 gene for prolipoprotein signal peptidase in *Escherichia coli*. *Mol Gen Genet* **192**: 10-  
677 14.

678 Yethon JA, Heinrichs DE, Monteiro MA, Perry MB, Whitfield C. 1998. Involvement of  
679 waaY, waaQ, and waaP in the modification of *Escherichia coli* lipopolysaccharide  
680 and their role in the formation of a stable outer membrane. *J Biol Chem* **273**: 26310-  
681 26316.

682 Yethon JA, Vinogradov E, Perry MB, Whitfield C. 2000. Mutation of the lipopolysaccharide  
683 core glycosyltransferase encoded by waaG destabilizes the outer membrane of  
684 *Escherichia coli* by interfering with core phosphorylation. *J Bacteriol* **182**: 5620-  
685 5623.

686 Yethon JA, Whitfield C. 2001. Purification and characterization of WaaP from *Escherichia*  
687 *coli*, a lipopolysaccharide kinase essential for outer membrane stability. *J Biol Chem*  
688 **276**: 5498-5504.

689 Zhang L, Dhillon P, Yan H, Farmer S, Hancock RE. 2000a. Interactions of bacterial  
690 cationic peptide antibiotics with outer and cytoplasmic membranes of *Pseudomonas*  
691 *aeruginosa*. *Antimicrob Agents Chemother* **44**: 3317-3321.

692 Zhang L, Scott MG, Yan H, Mayer LD, Hancock RE. 2000b. Interaction of polyphemusin I  
693 and structural analogs with bacterial membranes, lipopolysaccharide, and lipid  
694 monolayers. *Biochemistry* **39**: 14504-14514.

695

## FIGURE TITLES AND LEGENDS

### Figure 1. PMB causes a specific OM defect.

(A) PMB at 0.5  $\mu\text{g/ml}$  causes a slight OM permeability defect based on increased uptake and fluorescence of NPN dye. Graphs represent mean normalized end-point fluorescence  $\pm$  SD,  $n=3$ . (B) This concentration of PMB does not cause depolarization of the IM. Unlike gramicidin, PMB is unable to release PMF-dependent DiSC3(5) dye. Graphs represent mean normalized end-point fluorescence  $\pm$  SD,  $n=3$ . (C) Kinetics of Rcs induction upon PMB and Glb treatment at the mRNA (upper panel) and protein level (lower panel). Induction was monitored using a chromosomal *PrprA-lacZ* reporter by qRT-PCR or  $\beta$ -galactosidase assays. For mRNA quantification, graphs represent relative expression values normalized to a no treatment control for each time point  $\pm$  SD.  $\beta$ -galactosidase activity represent mean  $V_{\text{max}}$  normalized to OD600,  $\pm$  SEM,  $n=3$ . (D) PMB induces Rcs but not the Cpx or SigmaE stress responses. Induction was monitored by following the relative expression of *PrprA-lacZ* (Rcs), *cpxP* (Cpx) or *rpoE* (SigmaE) by qRT-PCR. Graphs represent mean  $\pm$  SEM,  $n=3$ . (E) PMB does not cause OMP assembly defects based on immunoblot analysis.

### Figure 2. The PMB-induced Rcs response is independent of *de novo* protein synthesis.

Cell cultures were pretreated with Ksg to inhibit protein synthesis for 15 mins prior to addition of PMB or Glb. Rcs induction was then monitored by qRT-PCR. Graphs represent relative expression values normalized to a no treatment control for each time point, mean  $\pm$  SEM,  $n=3$ .

### Figure 3. RcsF/OMP complexes are required for sensing OM stress.

(A) Topology and assembly pathway of RcsF/OMP complexes (based on (14)). The lipidated N-terminus of RcsF is anchored in the outer leaflet of the OM exposing residues 16-49 on the cell surface. The transmembrane segment (residues 50-65) of RcsF is threaded through the lumen of the OMP exposing the C-terminal domain in the periplasm. RcsF/OMP complexes are assembled by the Bam machine. Not all OMPs are complexed with RcsF. The effect of different mutants used in this study on the assembly of RcsF/OMP complexes is shown. (B) The effect of *ompA*, *bamE* and *rcsF\_A55Y* mutations on RcsF crosslinking to BamA and OmpA (upper panel) and the total RcsF, BamA and OmpA levels based on immunoblot analysis. (C) The *ompA*, *bamE* and *rcsF\_A55Y* mutants do not respond to PMB (upper panel) but respond to Glb (lower panel) treatment based on expression of *PrprA-lacZ*. Graphs represent mean  $\beta$ -galactosidase activity  $\pm$  SEM,  $n=3$ . (D) The *bamE* and *rcsF\_A55Y* mutants result in decreased *PrprA-lacZ*. Graphs represent mean  $\beta$ -galactosidase activity  $\pm$  SEM,  $n=3$ . Corresponding OD600 graphs and untreated controls are shown in Figure 3 – Figure supplement 1.

### Figure 4. RcsF senses alteration in LPS structure.

A) Structure and biosynthesis of *E. coli* K-12 LPS according to (Raetz and Whitfield 2002). Non-essential enzymes are shown in bold. (B) The effect of mutations in non-essential genes in the LPS biosynthesis pathway on Rcs induction based on *PrprA-lacZ* expression. (C and D) OM permeability is not a physiological inducing signal for Rcs. (C) Mutations that cause defects in asymmetry (*pldA mlaA*) or LPS export (*lptD4213* and *lptE\_R91D K136D*) do not induce Rcs. RcsF is not generally inhibited in these strains because Rcs can still be induced by introducing the *waaP* mutation. (D) Mutations *pldA mlaA*, *lptD42133* and *lptE\_R91D K136D* confer OM permeability defects (see text for references) assayed by plating 10-fold serial dilutions of overnight cultures onto LB plates supplemented with antibiotics or detergents. Note, arabinose (Ara) is required for growth of *lptE\_R91D K136D* mutant. (E) The addition of  $Mg^{2+}$  reduces Rcs signaling in the *waaP* background in a *phoP*-independent manner. (F) Lipid-truncated PMB derivative, PMBN, induces Rcs in concentration-dependent manner. Graphs B, C, E and F represent mean  $\beta$ -galactosidase activity  $\pm$  SEM, n=3

**Figure 5. Positive charge of the surface-exposed region of RcsF is required for LPS-sensing.**

(A) Amino acid sequences and total charge of the surface exposed domain of RcsF\_WT and the charge substitution mutant RcsF\_A5. Positively charged residues (Lys and Arg) which were substituted by Ala are underlined. (B) Charge substitution mutations do not affect RcsF crosslinking to BamA and OmpA. (C) The *rcsF\_A5* mutant does not respond to PMB (upper panel) but does respond to Glb (lower panel) treatment based on expression of a *PrprA-lacZ* reporter analyzed by beta-galactosidase assay. (D) The *rcsF\_A5* mutant results in decreased *PrprA-lacZ* expression in the *waaP* background. Graphs C and D represent mean  $\beta$ -galactosidase activity  $\pm$  SEM, n=3. Corresponding OD600 graphs and untreated controls are shown in Figure 5 – Figure supplement 1.

## FIGURE SUPPLEMENTS

### Figure 1 – figure supplement 1.

Glb induces Rcs but not the SigmaE stress response.

Induction was monitored by following the expression of *PrprA-lacZ* (Rcs) and *rpoE* (SigmaE) by qRT-PCR. Graphs represent relative expression values normalized to a no treatment control for each time point, mean +/- SEM, n=3

### Figure 3 – figure supplement 1.

(A) MIC values for the RcsF/OMP assembly defective strains.

(B) Kinetics of *PrprA-lacZ* expression in RcsF/OMP assembly defective strains upon treatment with PMB, Glb (same as Figure 3C) and untreated controls together with corresponding growth curves. Graphs represent mean  $\beta$ -galactosidase activity or OD600 +/- SEM, n=3

### Figure 3 – figure supplement 2.

#### (A) Growth curves of the assembly mutants in *waaP* background.

Strains were grown at 37° C in 1 ml of LB in 24 well plate and OD600 was monitored with a Biotek Synergy 1 plate reader. Note, *waaP ompA* strains display a synthetic growth phenotype. Graphs represent mean OD600 +/- SEM.

#### (B) Plate phenotype of the assembly mutants in the WT and *waaP* backgrounds.

Strains were grown on LB agar at 37° C overnight. Note, that the *waaP* mutation confers a RcsF-dependent mucoid phenotype. Introduction of a *bamE* mutation in *waaP* strain results in a loss of this phenotype. pZS21::*rscF* complements *waaP rcsF* mutant but does not confer a gain-of-function phenotype in the WT background. pZS21::*rscF\_A55Y* failed to complement the mucoid phenotype.

### Figure 5 – figure supplement 1.

Kinetics of *PrprA-lacZ* expression in RcsF/OMP charge substitution strains upon treatment with PMB, Glb (same as Figure 5C) and untreated controls together with corresponding growth curves. Graphs represent mean  $\beta$ -galactosidase activity or OD600 +/- SEM, n=3

### Figure 5 – figure supplement 2.

#### Plate phenotype of the charge substitution mutant in the WT and *waaP* background.

Strains were grown on LB agar at 37° C overnight. Note, that the *waaP* mutation confers a RcsF-dependent mucoid phenotype. pZS21::*rscF* complements *waaP rcsF* mutant but does not confer gain-of-function phenotype in the WT background. pZS21::*rscF\_A5* failed to complement mucoid phenotype.

804 **SUPPLEMENTARY FILE 1**

805 **Strains used in this study**

806

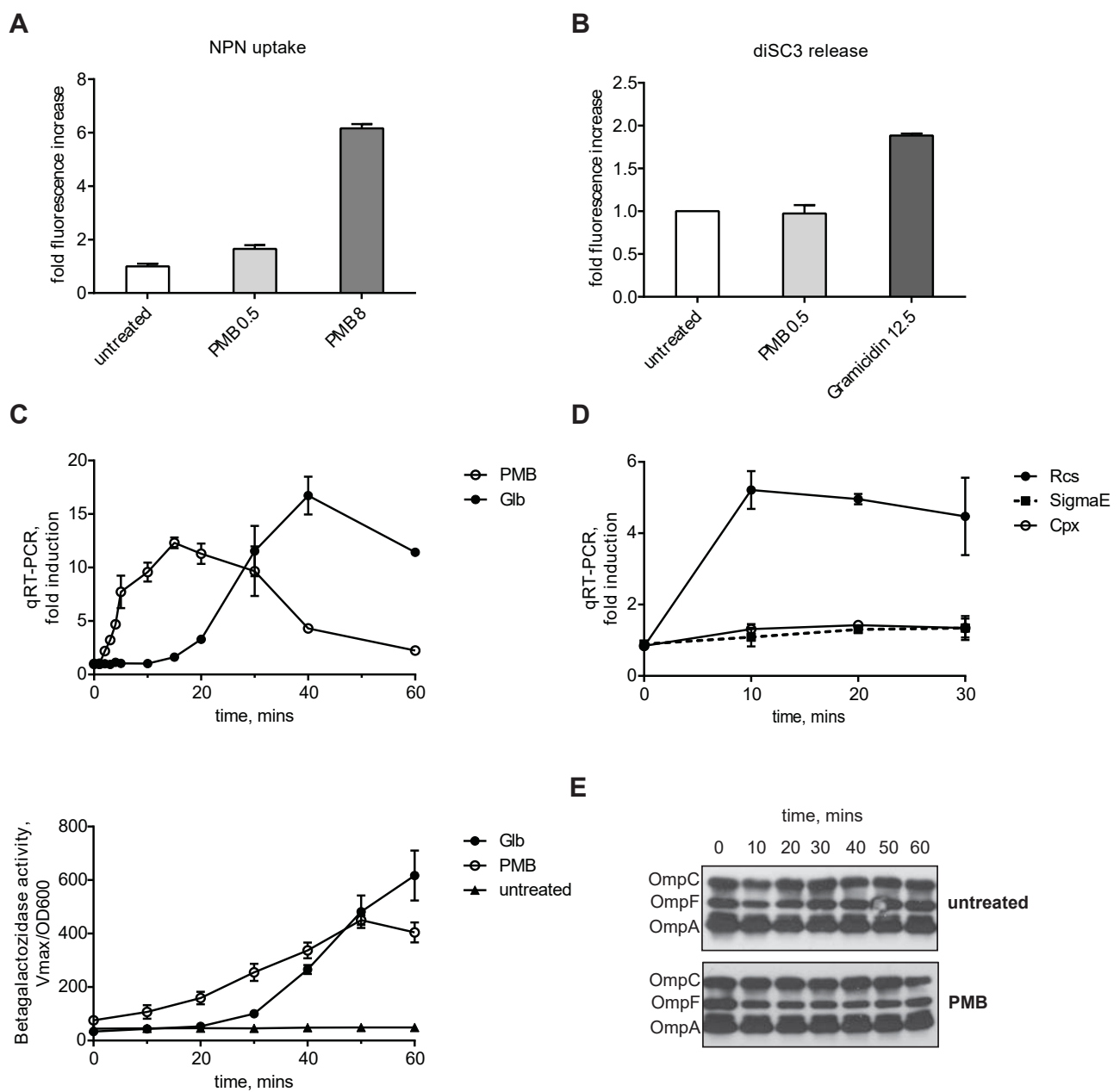


Figure 1

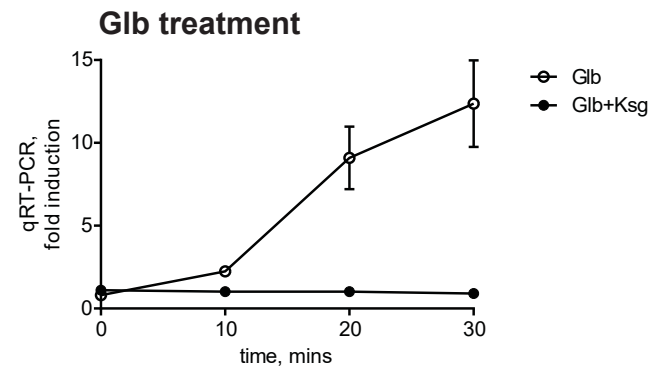
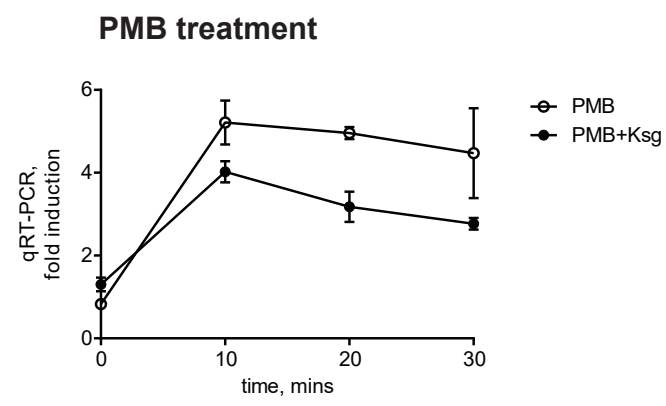


Figure 2

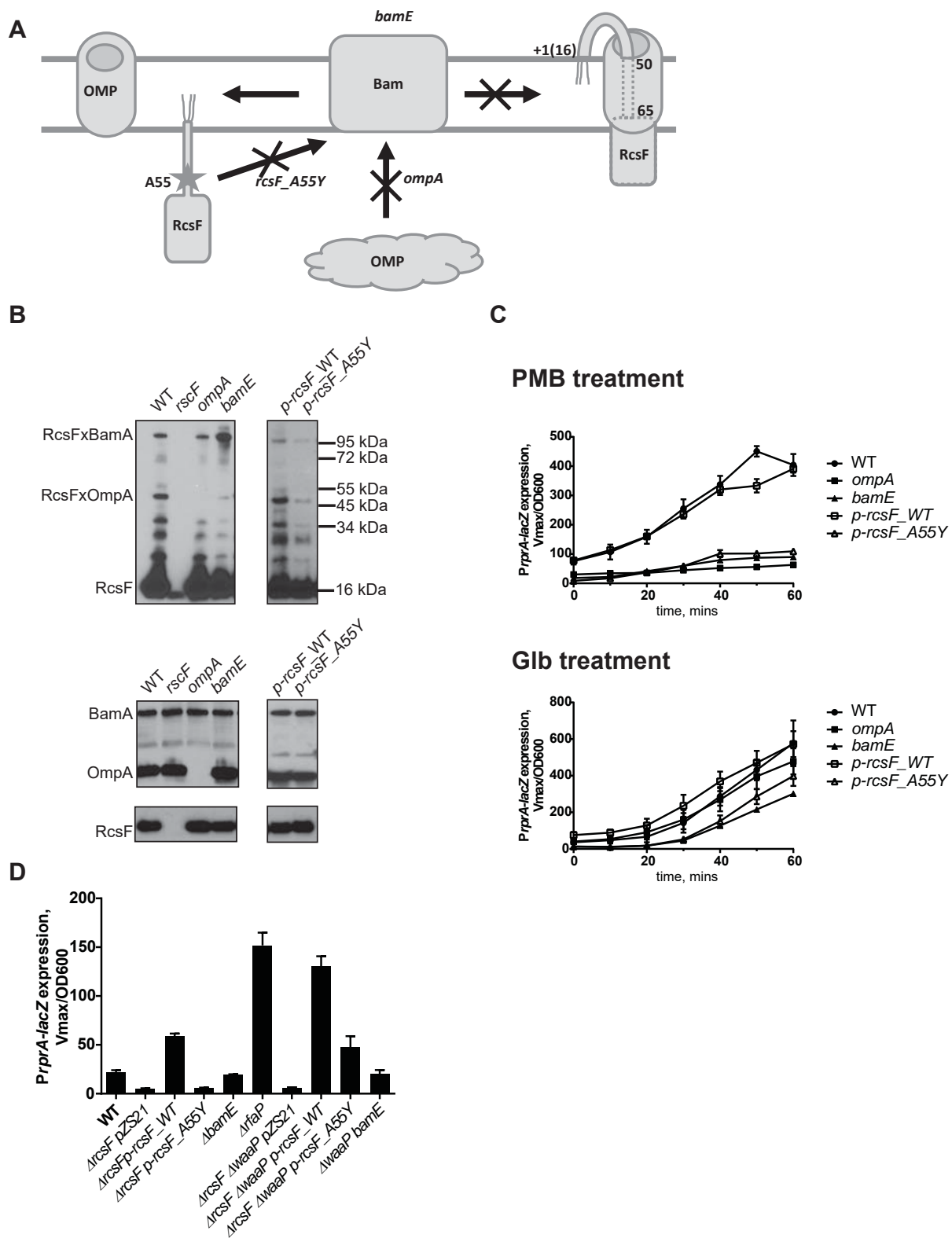
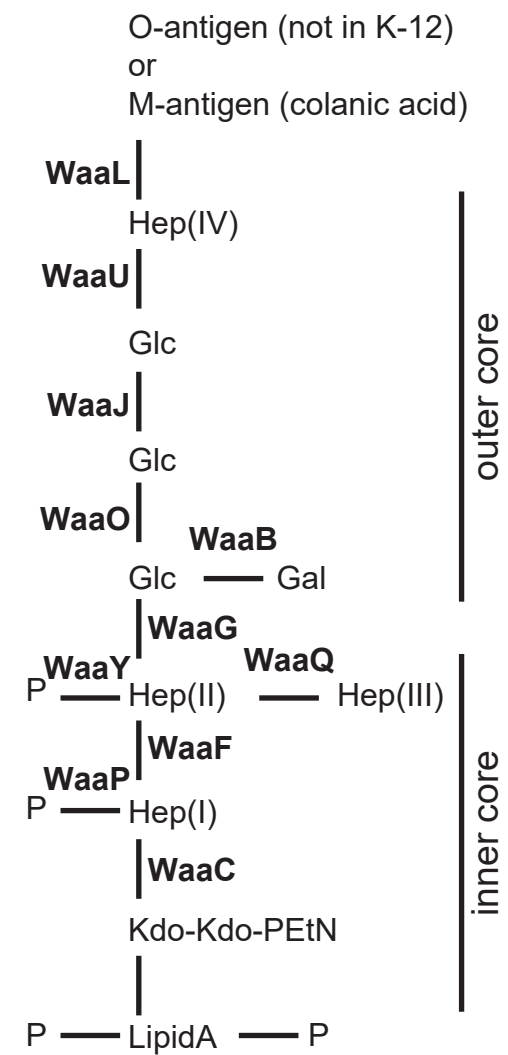


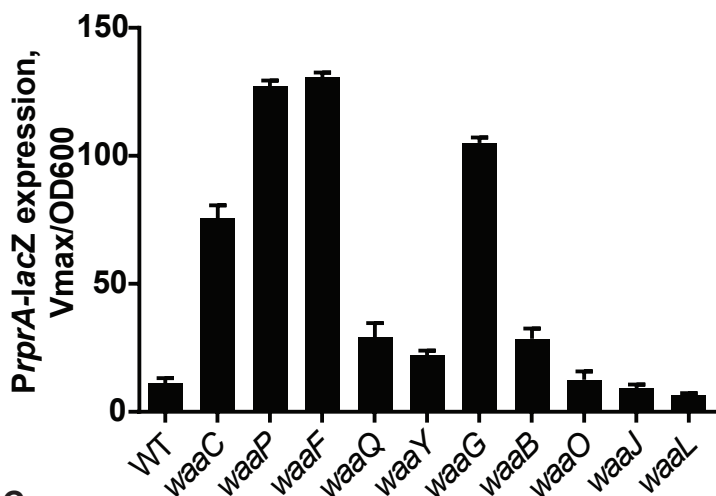
Figure 3



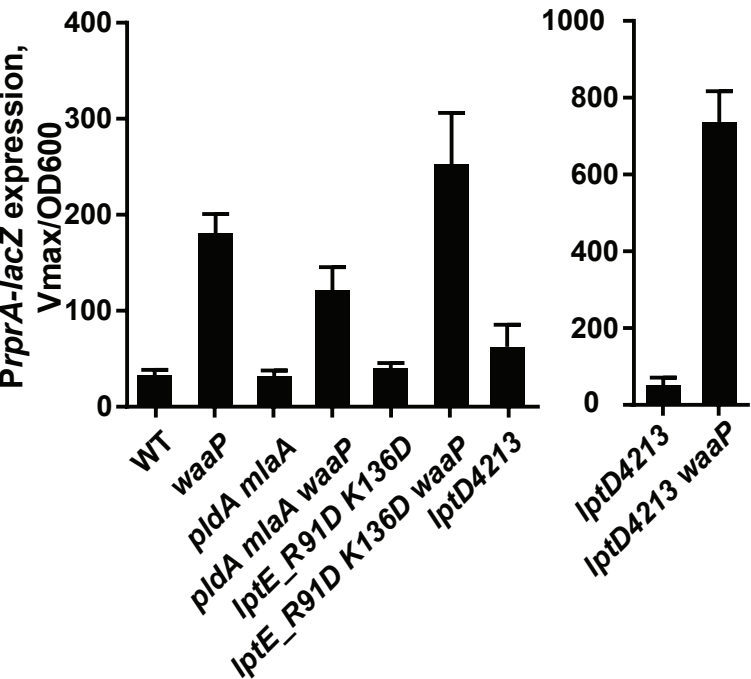
A



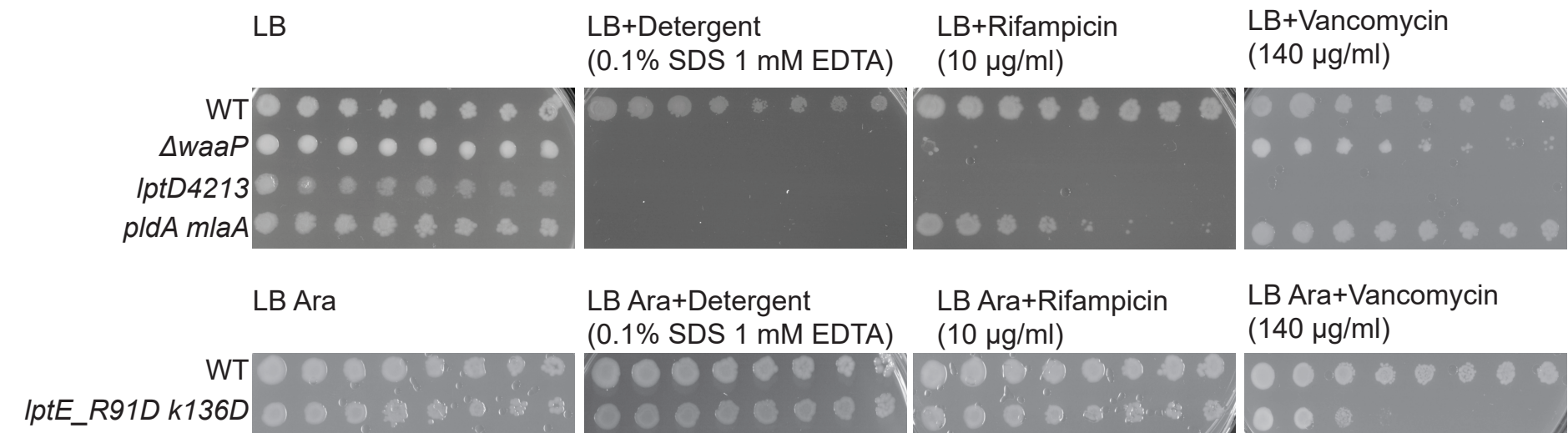
B



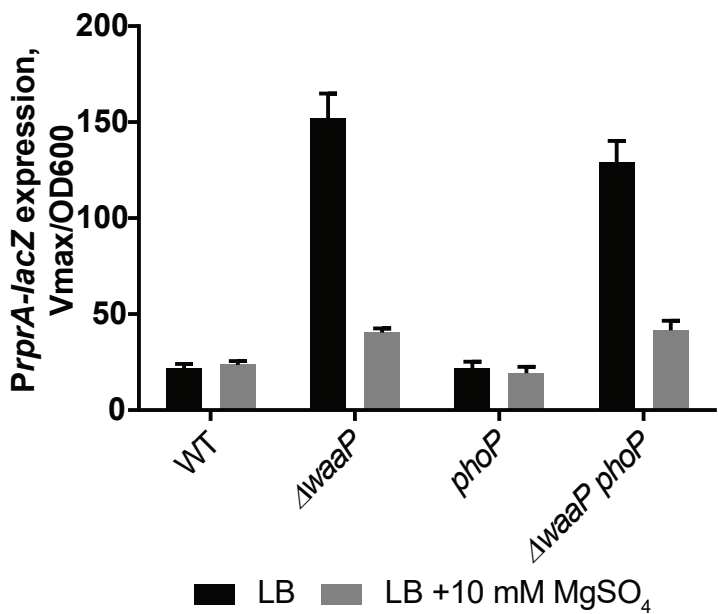
C



D



E



F

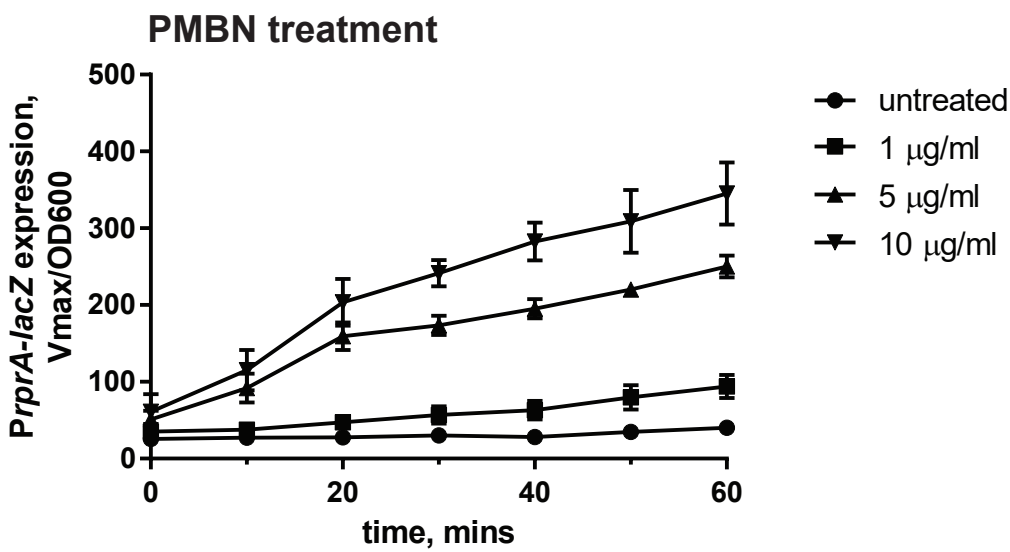


Figure 4

Figure 5